Temperature and pressure dependence of Raman-active phonons of $CaMoO_4$: an anharmonicity study



2002 J. Phys.: Condens. Matter 14 8925

(http://iopscience.iop.org/0953-8984/14/39/302)

INSTITUTE OF PHYSICS PUBLISHING JOURNAL OF PHYSICS: CONDENSED MATTER

J. Phys.: Condens. Matter **14** (2002) 8925–8938 PII: S0953-8984(02)33989-4

# Temperature and pressure dependence of Raman-active phonons of $CaMoO_4$: an anharmonicity study

**E Sarantopoulou[1,4], C Raptis[1], S Ves[2], D Christofilos[3] and G A Kourouklis[3]**

[1] Department of Physics, National Technical University of Athens, GR-15780 Athens, Greece
[2] Department of Physics, Aristotle University, GR-54006 Thessaloniki, Greece
[3] Division of Physics, School of Technology, Aristotle University, GR-54006 Thessaloniki, Greece

Received 19 February 2002, in final form 30 July 2002
Published 19 September 2002
Online at stacks.iop.org/JPhysCM/14/8925

**Abstract**

The Raman spectra of tetragonal $CaMoO_4$ (scheelite structure, $C_{4h}^6$ space group) have been measured in the temperature range 12–1300 K. At high temperatures, the frequency and linewidth of all Raman-active phonons vary almost linearly with temperature, indicating that the three-phonon decay processes are dominant over the four-phonon ones. All Raman phonons display normal negative $(\partial\omega/\partial T)$ slopes throughout the temperature range, except for the lowest-frequency $B_g$ phonon at 111.5 $cm^{-1}$ which is almost temperature independent in the region 12–400 K, but then for $T > 400$ K it shows a slight (normal) softening with temperature. The reduced $(\partial\omega/\partial T)/\omega$ slopes of the internal modes (vibrations of atoms within the tetrahedral $MoO_4^{2-}$ units) are an order of magnitude smaller than the respective slopes of the external ones (pure lattice modes). There are no discontinuities or sharp changes of slope in the $\omega(T)$ plots, implying that $CaMoO_4$ remains stable over the entire temperature range. Combining the temperature-dependent Raman data of this work and the previously reported pressure-dependent Raman data on this crystal (Christofilos D, Kourouklis G A and Ves S 1995 *J. Phys. Chem. Solids* **56** 1125), as well as the thermal expansion coefficient $\beta(T)$ and compressibility $\kappa(T)$ data, it has been possible to separate and evaluate quantitatively the volume (expansion) $\Delta\omega_{vol}$ and the pure temperature (anharmonic) $\Delta\omega_{anh}$ contributions to the total $\Delta\omega_{tot}$ shift of phonons with temperature. It has been found that for most phonons at high temperatures, the volume effect is greater than the pure temperature one, thus indicating that most of the bonds in $CaMoO_4$ are predominantly ionic in character.

[4] Present address: Institute of Theoretical and Physical Chemistry, National Hellenic Research Foundation, GR-11635 Athens, Greece.

0953-8984/02/398925+14$30.00  

## 1. Introduction

Like most molybdate and tungstate compounds, at ambient conditions $CaMoO_4$ has the tetragonal scheelite ($CaWO_4$) type of structure ($C_{4h}^6$ space group) with two molecules in the unit cell [1, 2]. These crystalline compounds, and in particular $CaMoO_4$, have been extensively used as host materials for optically active rare-earth ions and, hence, for solid-state laser applications [3]. Therefore, knowledge of their structural stability range under conditions of variable temperature or pressure is important for such applications. Raman spectroscopy constitutes a reliable technique for monitoring the structural stability of materials under such variable conditions and has been extensively used for studying the structure of these scheelite-type compounds under variable pressure [4–8]. On the temperature dependence side, three Raman studies have been published to date, one [9] on tungstates at low temperatures (10–300 K), another on the linewidth of Raman phonons of $CaWO_4$ [10] in the range 77–771 K and a recent one [11] on tungstates and molybdates (including $CaMoO_4$) from 77 K up to the melting point in which emphasis is given to the temperature dependence of the linewidth of Raman phonons.

In previous Raman studies [2, 8, 12, 13] of $CaMoO_4$ at ambient conditions, assignment of its Raman-active phonons has been made with reference to the various symmetries and atomic motions; these studies [2, 8, 12, 13] have also helped towards a better understanding of its structure. It has been established that in scheelite $MXO_4$ (M = Ca, Sr, Ba; X = W, Mo) crystals [1, 2, 8, 12–14], four oxygen atoms are in tetrahedral coordination around an X atom, thus forming rather tightly bound molecular $XO_4^{2-}$ anions which are bonded to the metal $M^{2+}$ cations in the lattice via relatively weak long-range ionic forces. As a result of this difference in force constant between the two types of bond, the vibrational frequencies of the 'internal' modes within the $XO_4^{2-}$ anions are greater than those of the 'external' modes corresponding to vibrations between lattice ions (pure lattice modes).

Group theory predicts 13 Raman modes for the $C_{4h}^6$ structure of $CaMoO_4$ with $A_g$, $B_g$, or doubly degenerate $E_g$ symmetries corresponding to the following polarizability tensors [2]:

$$A_g = \begin{pmatrix} a & 0 & 0 \\ 0 & a & 0 \\ 0 & 0 & b \end{pmatrix}, \qquad B_g = \begin{pmatrix} c & d & 0 \\ d & -c & 0 \\ 0 & 0 & 0 \end{pmatrix}, \qquad E_g = \begin{pmatrix} 0 & 0 & e \\ 0 & 0 & e \\ e & e & 0 \end{pmatrix}.$$

Seven of these modes ($2A_g + 3B_g + 2E_g$) are internal in the $MoO_4$ tetrahedra, while the other six ($1A_g + 2B_g + 3E_g$) are external pure lattice modes (translational and rotational motions between ions in the lattice).

In a previous high-pressure Raman study by Christofilos *et al* [8] of $CaMoO_4$ up to 23 GPa, it was reported that almost all Raman modes exhibit normal positive $\partial\omega/\partial P$ slopes, except that of the lowest-frequency $B_g$ phonon at 111.5 $cm^{-1}$ (associated with $MoO_4^{2-}$–$MoO_4^{2-}$ motions along the *c*-axis) which shows a negative $\partial\omega/\partial P$ slope up to 8.2 GPa and a normal positive one above this pressure. Also, in the same study [8], discontinuous $\partial\omega/\partial P$ slope variations at 8.2 and 15 GPa indicate that $CaMoO_4$ undergoes structural changes at these pressures.

In this article we report the temperature dependence of the Raman-active phonons of $CaMoO_4$ over the region 12–1300 K. The motivation for this work is threefold:

(i) to assess the structural stability of the material with temperature;
(ii) to investigate the behaviour with temperature of the lowest-frequency phonon which shows abnormal pressure dependence [8]; and, finally,
(iii) in combination with pressure-dependent Raman data published before [8], to carry out an anharmonicity analysis in which the contributions of the volume thermal expansion and the pure temperature effects to the total observed frequency shifts (with temperature) can be evaluated and compared.

## 2. Experimental procedures

Single oriented crystals of $CaMoO_4$ having rectangular polished faces with a typical dimension of ∼6 mm were used in this study. For the low-$T$ experiments (12–300 K), the sample was placed inside a closed-cycle He cryostat, while the high-$T$ experiments (300–1300 K) were carried out with the use of a vacuum-operated furnace of very low $T$-gradients [15]; in the latter experiments, the sample was held inside a silica cell which was linked, via another vacuum line, to an argon gas cylinder so that the measurements were performed in inert atmosphere. The sample temperature was monitored using thermocouples placed very close to the sample with an accuracy of ∼1 K at low $T$ and ∼3 K at high $T$. All spectra (both at low and high $T$) were recorded using a 90° scattering geometry. Polarized Raman spectra of $CaMoO_4$ were measured in order to assign the observed phonons to the symmetry species of the crystal class, and to resolve (mainly at high $T$) overlapping phonon lines of different symmetries. However, most of the recorded spectra were unpolarized; this was achieved by setting a mixed polarization for the incident laser beam and removing the analyser from the entrance slit of the monochromator.

The 488 nm line of an $Ar^+$ laser at a power of ∼150 mW was used for the excitation of Raman spectra. The scattered light was analysed by a SPEX 14018 model double monochromator and detected by a cooled photomultiplier. The spectral resolution was 1 and 2 $cm^{-1}$ at low and high $T$, respectively.

## 3. Results and discussion

The Raman spectra of $CaMoO_4$ in this work at ambient conditions are in good agreement with those of previous studies [2, 8, 12, 13] and the agreement applies to both the frequencies of Raman modes (within small margins of deviation) and the symmetry assignment of these modes. The frequencies $\omega_{300\,K}$ of all Raman phonons of $CaMoO_4$ measured at ambient conditions are given in table 1 along with their symmetries and other relevant quantities and parameters which are discussed below. The six lower-frequency bands ($\omega \leqslant 267$ $cm^{-1}$) correspond to the 'external' modes, while the seven higher-frequency bands ($\omega \geqslant 321.5$ $cm^{-1}$) correspond to the 'internal' ones [2, 8].

### *3.1. Temperature dependence of the Raman modes of $CaMoO_4$*

Typical unpolarized Raman spectra of $CaMoO_4$ at four temperatures (12, 295, 735 and 1260 K) are shown in figure 1. The temperature dependence of the Raman spectra in this work is in good agreement with that in a previous relevant work [11] on $CaMoO_4$. The mixed polarization configuration used for these spectra allowed the simultaneous observation of all 13 Raman modes of different symmetries. At the lowest $T$ all phonons are clearly resolved, but at elevated temperatures some nearby Raman bands do not resolve in the unpolarized spectra because of $T$-induced broadening and, for this reason, separate polarized spectra were recorded around the relevant spectral regions in order to distinguish the phonon species.

The frequencies of the Raman peaks observed have been plotted against temperature and nearly all show a normal softening with increasing $T$. The one exception is the lowest-frequency $B_g$ phonon at 111.5 $cm^{-1}$ (figure 2), which shows appreciable change in the region 12–400 K, although it too softens slightly at higher temperatures. As representative examples, the frequency versus temperature plots for two more phonons are given in figure 3, one for the external $A_g$ mode at 204.5 and the other for the internal $E_g$ mode at 792 $cm^{-1}$. The experimental

**Table 1.** Frequencies (at ambient conditions), symmetries and fitting parameters in equations (1) and (2) for the frequency–temperature (figures 2 and 3) and linewidth–temperature (figure 4) plots of the Raman-active phonons of $CaMoO_4$.

| $\omega_{300\,K}$ ($cm^{-1}$) | $\omega(0)$ ($cm^{-1}$) | $\omega_0$ ($cm^{-1}$) | $A$ ($cm^{-1}$) | $B$ ($cm^{-1}$) | $\Gamma_0$ ($cm^{-1}$) | $C$ ($cm^{-1}$) | $D$ ($cm^{-1}$) |
|---|---|---|---|---|---|---|---|
| 111.5 ($B_g$) | 111.5 ± 0.1 | 111.5 ± 0.1 | 0.026 | −0.0016 | 0.60 | 0.25 | 0.000 01 |
| | | | ±0.011 | ±0.0002 | ±0.06 | ±0.01 | ±0.000 1 |
| 143.0 ($E_g$) | 145.8 ±0.1 | 146.4 ± 0.1 | −0.597 | −0.0034 | 0.46 | 0.33 | 0.000 6 |
| | | | ±0.013 | ±0.0003 | ±0.08 | ±0.02 | ±0.000 3 |
| 189.5 ($E_g$) | 193.3 ± 0.2 | 194.4 ± 0.2 | −1.100 | −0.007 | 1.58 | 0.62 | 0.005 |
| | | | ±0.053 | ±0.002 | ±0.21 | ±0.06 | ±0.001 |
| 204.5 ($A_g$) | 209.3 ± 0.2 | 210.8 ± 0.1 | −1.545 | −0.018 | 2.25 | 0.32 | 0.025 |
| | | | ±0.042 | ±0.002 | ±0.48 | ±0.16 | ±0.004 |
| 214.0 ($B_g$) | 219.6 ± 0.7 | 221.9 ± 0.5 | −2.28 | −0.021 | — | — | — |
| | | | ±0.19 | ±0.007 | | | |
| 267.0 ($E_g$) | 270.9 ± 0.5 | 272.8 ± 0.3 | −1.83 | −0.023 | 2.24 | 1.54 | 0.002 |
| | | | ±0.15 | ±0.007 | ±0.28 | ±0.03 | ±0.003 |
| 321.5 ($A_g$) | 322.8 ± 0.2 | 323.3 ± 0.1 | −0.48 | −0.034 | 2.09 | 2.31 | 0.009 |
| | | | ±0.07 | ±0.004 | ±0.18 | ±0.13 | ±0.007 |
| 327.5 ($B_g$) | 330.4 ± 0.3 | 332.1 ± 0.2 | ±1.72 | 0.019 | 4.10 | 3.13 | −0.009 |
| | | | ±0.12 | ±0.008 | ±0.25 | ±0.21 | ±0.011 |
| 391.0 ($B_g$) | 391.6 ± 0.2 | 392.1 ± 0.1 | −0.47 | −0.034 | 1.99 | 1.40 | −0.008 |
| | | | ±0.07 | ±0.005 | ±0.06 | ±0.04 | ±0.002 |
| 402.5 ($E_g$) | 403.6 ± 0.3 | 404.7 ± 0.2 | −1.14 | −0.021 | 4.14 | 2.25 | −0.000 1 |
| | | | ±0.11 | ±0.008 | ±0.27 | ±0.07 | ±0.000 8 |
| 792.0 ($E_g$) | 793.5 ± 0.5 | 797.9 ± 0.3 | −4.43 | −0.02 | 2.66 | 3.33 | 0.034 |
| | | | ±0.23 | ±0.03 | ±0.22 | ±0.48 | ±0.045 |
| 845.5 ($B_g$) | 847.2 ± 0.4 | 853.1 ± 0.2 | −5.91 | −0.02 | 2.24 | 2.25 | 0.107 |
| | | | ±0.21 | ±0.01 | ±0.06 | ±0.14 | ±0.013 |
| 877.0 ($A_g$) | 878.0 ± 0.6 | 883.5 ± 0.3 | −5.65 | 0.18 | 2.34 | 5.59 | 0.034 |
| | | | ±0.31 | ±0.04 | ±0.08 | ±0.20 | ±0.020 |

points of the frequency–$T$ plots of all 13 phonons have been best fitted to the expression

$$\omega(T) = \omega_0 + A\left(1 + \frac{2}{e^x - 1}\right) + B\left(1 + \frac{3}{e^y - 1} + \frac{3}{(e^y - 1)^2}\right) \tag{1}$$

which has been used by Balkanski *et al* [16] for the anharmonic decay of the LO Raman mode of crystalline Si at high $T$; the exponents $x = h\omega_0/2k_BT$, $y = h\omega_0/3k_BT$ refer to terms of three- and four-phonon decay processes contributing to the frequency shift with $T$, respectively. The solid curves in figures 2 and 3 represent the fittings of the experimental points to the function of equation (1) which is not merely a suitable function for fitting the experimental data, but also has a physical meaning as it is based on a theory [17] which has dealt successfully with anharmonic decay of a phonon (at high $T$) to other phonons of lower frequencies. The fitting values for the parameters $\omega_0$, $A$ and $B$ of the expression of equation (1) are given in table 1 for all phonons. Also, in the same table the extrapolated frequency values $\omega(0) = \omega_0 + A + B$ are given as obtained from equation (1) for $T = 0$.

The linewidth for all phonons (full width at half-maximum (FWHM)) has also been plotted against $T$ and the plots for two phonons, $B_g$ at 111.5 $cm^{-1}$ and $A_g$ at 877 $cm^{-1}$, are shown in figure 4. The data points of the linewidth–$T$ plots for 12 (out of 13) phonons have been best fitted to the following expression [16]:

$$\Gamma(T) = \Gamma_0 + C\left(1 + \frac{2}{e^x - 1}\right) + D\left(1 + \frac{3}{e^y - 1} + \frac{3}{(e^y - 1)^2}\right) \tag{2}$$

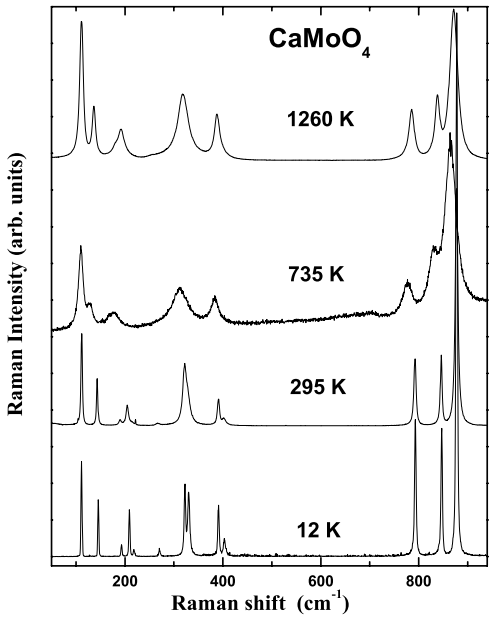


**Figure 1.** Unpolarized Raman spectra of $CaMoO_4$ at four temperatures in the range 12–1260 K in which all 13 Raman-active phonons are recorded.

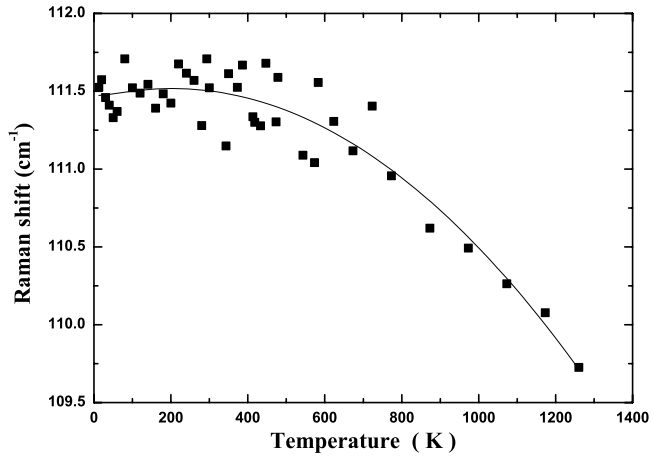


**Figure 2.** The temperature dependence of the frequency of the $B_g$ phonon at 111.5 $cm^{-1}$. The solid curve is a least-squares fitting of the experimental points to equation (1).

which is similar to equation (1) with contributions from both three- and four-phonon decay processes. A two-parameter fitting was used originally [16], without the constant term $\Gamma_0$. We have found, though, that much better fittings are obtained using three parameters, rather than two; this procedure can be justified in terms of a constant, underlying broadening for each phonon due to mechanisms other than the anharmonic phonon decay, such as defects and impurities. All linewidths have been corrected by taking into consideration the broadening of the recorded spectral lines due to the spectrometer. Again, the solid lines in the $\Gamma$–$T$ plots of figure 4 are the best fittings of the experimental data to the function of equation (2). It was not

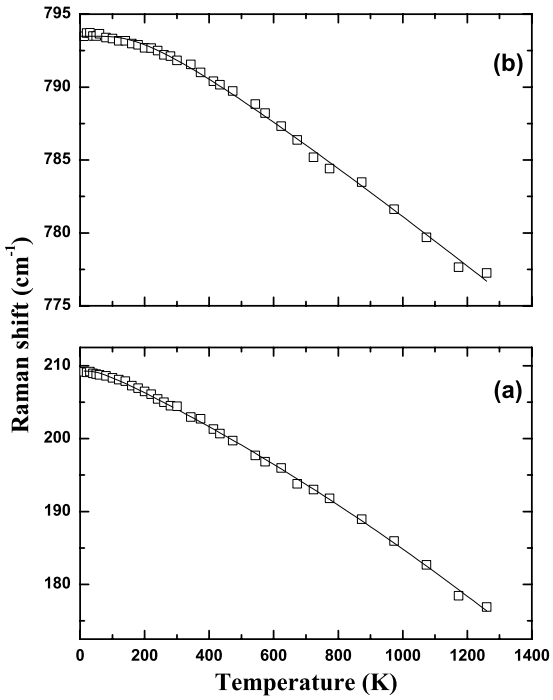


**Figure 3.** The temperature dependence of the frequencies of the $A_g$ (a) and $E_g$ (b) phonons at 204.5 and 792 cm$^{-1}$, respectively. The solid curves are least-squares fittings of the experimental points to equation (1).

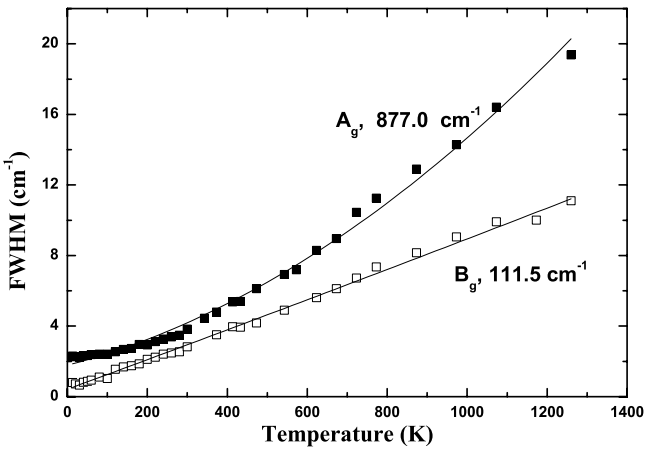


**Figure 4.** FWHMs of the $B_g$ and $A_g$ phonons at 111.5 and 877 cm$^{-1}$, respectively. The solid curves are least-squares fittings of the experimental points to equation (2).

possible to produce any reliable linewidth fitting for the weak $B_g$ phonon at 214 cm$^{-1}$ because of a very strong spread of points at high temperatures. The values of the fitting parameters $\Gamma_0$, $C$ and $D$ for 12 phonons are given in table 1.

From the fittings of the frequency versus $T$ plots we have obtained the slopes $\partial\omega/\partial T$ and their values for $T = 300$ K are given in table 2. For comparison, and since this slope is

**Table 2.** Pressure and temperature slopes and degree of linewidth broadening for Raman-active phonons of $CaMoO_4$. The pressure slopes are from [8].

| Phonon frequency $\omega_{300\,K}$ ($cm^{-1}$) | $(\partial\omega/\partial T)_{300\,K}$ ($cm^{-1}\,K^{-1}$) | $\{(\partial\omega/\partial T)/\omega\}_{300\,K}$ ($10^{-5}\,K^{-1}$) | $(\partial\omega/\partial P)_{300\,K}$ ($cm^{-1}\,GPa^{-1}$) | $(\Gamma_h - \Gamma_l)/\Gamma_l$ |
|---|---|---|---|---|
| 111.5 ($B_g$) | ∼0 (−0.0013 at 600 K) | ∼0 (−1.7 at 600 K) | −0.2 | 10.5 |
| 143.0 ($E_g$) | −0.013 | −9.1 | 1.9 | 18.0 |
| 189.5 ($E_g$) | −0.017 | −9.0 | 4.0 | 11.0 |
| 204.5 ($A_g$) | −0.023 | −11.2 | 3.7 | 12.0 |
| 214.0 ($B_g$) | −0.031 | −14.5 | 5.1 | — |
| 267.0 ($E_g$) | −0.021 | −7.9 | 6.5 | 10.0 |
| 321.5 ($A_g$) | −0.007 | −2.2 | 2.5 | 10.0 |
| 327.5 ($B_g$) | −0.012 | −3.7 | 4.2 | 6.5 |
| 391.0 ($B_g$) | −0.005 | −1.3 | 3.8 | 6.5 |
| 402.5 ($E_g$) | −0.008 | −2.0 | 4.6 | 4.5 |
| 792.0 ($E_g$) | −0.012 | −1.5 | 3.0 | 6.0 |
| 845.5 ($B_g$) | −0.014 | −1.7 | 2.1 | 5.0 |
| 877.0 ($B_g$) | −0.011 | −1.3 | 2.1 | 8.0 |

practically zero for the $B_g$ phonon at 111.5 $cm^{-1}$ at 300 K, the value of $\partial\omega/\partial T$ for this phonon at 600 K is also given in parentheses. Also, in table 2 the reduced slopes $(\partial\omega/\partial T)/\omega$ of all phonons are given for $T = 300$ K. Finally, the pressure slopes $\partial\omega/\partial P$ of $CaMoO_4$ from [8] are also shown in table 2; the latter slopes will be used in the anharmonicity analysis below.

We start the discussion from the $T$-dependence of the $B_g$ phonon at 111.5 $cm^{-1}$. As figure 2 shows, the frequency of this phonon is almost $T$-independent in the region 12–400 K. Bearing in mind that this phonon shows an abnormal softening [8] with increasing pressure (volume contraction), we conclude that the frequency shift due to the volume (expansion) effect in our $T$-dependent Raman measurements should be positive with increasing $T$, that is, the phonon should harden with $T$; therefore, the invariance of frequency of this phonon in the region 12–400 K implies that the volume effect is balanced (compensated) by the pure temperature effect which should be of opposite sign to the former. More details on this issue are given in the following sections which involve a quantitative anharmonic analysis. For $T > 400$ K, this phonon displays a slight softening which becomes almost linear above 600 K (figure 2). In fact, all phonons display a nearly linear dependence on $T$ above a certain threshold $T$ (see figures 2 and 3) which varies between 400 and 600 K, depending on the phonon, and this behaviour implies that the three-phonon decay processes (second term in the right-hand side of equation (1)) dominate their frequency shifts [16, 17]. This conclusion is further supported by the fact that the values of the parameter $A$ are much greater than those of parameter $B$ which are obtained by the fits to equation (1) (see table 1).

The linewidth of all phonons increases initially non-linearly with $T$ up to about 400 K, but for $T > 400$ K the linewidth dependence is almost linear (figure 4), showing again that the three-phonon-process contributions (cubic anharmonic terms) to the phonon broadening are dominant over the four-phonon ones (quartic anharmonic terms) [16, 17]. Again, confirmation that the three-phonon processes dominate the scattering at high temperatures is implied by the much larger values of the parameter $C$, in comparison to those of parameter $D$, in the fits to equation (2) (table 1). We consider the ratio $(\Gamma_h - \Gamma_l)/\Gamma_l$ as a quantitative measure of the phonon broadening, where $\Gamma_h$ and $\Gamma_l$ represent the linewidths at a high $T$ (=1000 K) and the lowest $T$ of measurement. The values of this ratio for all phonons are shown in table 2. It is apparent that the linewidth broadening is smaller for the high-frequency internal modes and this result is anticipated because of the stronger binding of atoms in the $MoO_4^{2-}$ units.

The $\partial\omega/\partial T$ slopes of the internal modes are on the whole lower than those of the external modes (table 2). A more representative quantity for comparisons of the bond strength corresponding to a mode is the reduced $(\partial\omega/\partial T)/\omega$ slope. These reduced slopes are also given in table 2 for all phonons, showing that the values for the high-frequency internal modes are almost an order of magnitude smaller than those of the external modes, thus confirming the stronger bonding (compared to the external pure lattice modes) within the $MoO_4^{2-}$ units. One notable exception to this general trend is the small slope of the $B_g$ phonon at 111.5 $cm^{-1}$. This can be understood in terms of an abnormal volume (expansion) effect whose contribution seems to strengthen the force constant of the $MoO_4^{2-}$–$MoO_4^{2-}$ vibration corresponding to this mode. This, in its turn, is concluded by the abnormal softening of the mode with pressure [8], i.e., the weakening of the force strength with volume contraction.

From the frequency–$T$ plots of all phonons (such as those of figures 2 and 3), there is no evidence of discontinuities or abrupt changes of slope which means that there are no phonon instabilities, thus implying that $CaMoO_4$ remains stable throughout the $T$-region of 12–1300 K.

### *3.2. Anharmonicity analysis*

*3.2.1. Outline of background theory—procedures of analysis.* It is well known [18–25] that in temperature-dependent Raman measurements performed on crystalline materials, the observed phonon frequency shifts are due to the combination of two effects:

(i) the volume expansion (implicit) effect which changes the atomic distances and, consequently, the force constants corresponding to the bonds; and
(ii) the pure temperature (explicit) effect related to anharmonic phonon interaction and decay to other phonons at high $T$.

For an isotropic crystal these contributions to the total shift can be separated and evaluated using the following expression:

$$\left(\frac{\partial\omega}{\partial T}\right)_P = -\frac{\beta(T)}{\kappa(T)}\left(\frac{\partial\omega}{\partial P}\right)_T + \left(\frac{\partial\omega}{\partial T}\right)_V \tag{3}$$

where $(\partial\omega/\partial T)_P$ is the (isobaric) rate of frequency change with $T$ as measured in $T$-dependent Raman experiments (total shift), $(\partial\omega/\partial P)_T$ is the (isothermal) change of frequency with pressure as determined in pressure-dependent Raman experiments (volume contraction), $\beta(T)$ is the volume thermal expansion coefficient and $\kappa(T)$ is the volume compressibility. The volume effect contribution is given by the first term on the right of equation (3), while the term $(\partial\omega/\partial T)_V$ is the (isochoric) change of frequency with $T$, representing the pure temperature (anharmonic) effect contribution, a quantity which cannot be measured directly but can be estimated from equation (3). Integration of equation (3) gives the total frequency shift:

$$\Delta\omega_{tot}(T) = \omega(0) - \omega(T) = \Delta\omega_{vol}(T) + \Delta\omega_{anh}(T) \tag{4a}$$

where $\Delta\omega_{vol}(T)$ and $\Delta\omega_{anh}(T)$ are the contributions to the shift due to the volume expansion and pure temperature effects, respectively. Writing equation (4*a*) as

$$\Delta\omega_{anh}(T) = \Delta\omega_{tot}(T) - \Delta\omega_{vol}(T) \tag{4b}$$

one can calculate the shift due to the pure temperature effect. The total frequency shifts $\Delta\omega_{tot}(T)$ are obtained using the $\omega(0)$ values from table 1 and the measured frequencies $\omega(T)$ from the $\omega$–$T$ plots (such as those of figures 2 and 3). The volume expansion-induced shifts have been obtained from the integral

$$\Delta\omega_{vol}(T) = -\int_0^T \frac{\beta(T')}{\kappa(T')}\left(\frac{\partial\omega}{\partial P}\right)_{T'} \mathrm{d}T \tag{5}$$

using the slopes $(\partial\omega/\partial P)_T$ measured by Christofilos *et al* [8] at 300 K for the scheelite phase of $CaMoO_4$ (that is, in the region between 1 atm and 8 GPa; see [8]). It has been reported [21, 22] that the slopes $(\partial\omega/\partial P)_T$ are almost $T$-independent in other dielectric crystals and, because of this, they have been taken as constant in the integral of equation (5).

As was mentioned above, the theory leading to equations (3) and (5) refers to isotropic crystals of cubic symmetry for which the phonon frequency is considered a function of volume and temperature: $\omega = \omega(V, T)$. In a uniaxial crystal, such as $CaMoO_4$, the ratio $c/a$ of the lattice parameters varies with temperature so the phonon frequency is a function of three variables in $T$-dependent measurements: $\omega = \omega(a, c, T)$. Recently, Perakis *et al* [24] have derived accurate expressions of equations (3) and (5) for uniaxial crystals and applied them in the case of tetragonal $MgF_2$; it has been found [24] that in the case of $MgF_2$ for $T > 200$ K, the volume contribution calculated by the isotropic approximation of equation (5) differs by only 5–10% (depending on the phonon) from that calculated by the accurate expression [24] obtained for uniaxial crystals. It should be pointed out that application of the accurate approach is possible only when uniaxial stress Raman data are available. In the absence of such data for $CaMoO_4$, calculations of the two contributions to the phonon frequency shifts will be carried out using the isotropic approximation (equations (3) and (5)).

*3.2.2. Thermal expansion coefficient and compressibility of $CaMoO_4$.* The volume thermal expansion coefficient of $CaMoO_4$ has been determined from measurements [26] of the lattice constants $a$ and $c$ in the $T$-region 300–620 K using the formula

$$\beta(T) = \frac{2}{a(T)}\frac{\Delta a(T)}{\Delta T} + \frac{1}{c(T)}\frac{\Delta c(T)}{\Delta T} \tag{6}$$

which is valid for uniaxial crystals. Outside this $T$-region, there are no data available of $\beta(T)$ for $CaMoO_4$ originating from direct measurements of lattice parameters and, because of this, we have used Debye temperature data [27] corresponding to isomorphous $CaWO_4$ over the region 4.2–300 K in order to calculate $\beta(T)$ for $CaMoO_4$; matching of the two sets of data over the two $T$-regions was done by normalization of the Debye-derived value of $\beta(T)$ of $CaWO_4$ and that of $CaMoO_4$ obtained from equation (6) at 300 K. The Debye-derived values of $\beta(T)$ were calculated from the formula [25]

$$\beta(T) = \beta_\infty D(\xi) = \beta_\infty D(\Theta_D/T) \tag{7}$$

where

$$D(\xi) = \frac{3}{\xi^3}\int_0^\xi \frac{x^4}{(e^x - 1)^2}\,dx \tag{8}$$

is the Debye integral and $\beta_\infty = \beta(300)/D(\Theta_D/300)$ represents the high-$T$ limiting value of $\beta(T)$. Combination of the experimental values [26] for $\beta(T)$ obtained from equation (6) and the estimated ones [25] from equations (7) and (8) has allowed us to fit all these points to the formula [23–25]

$$\beta(T) = (E/T + F/T^2)\sinh^{-2}(T_0/T) \tag{9}$$

and the result of this fitting is shown in figure 5(a). Fitting values for the parameters $E$, $F$ and $T_0$ are given in table 3. Values of $\beta(T)$ for $CaMoO_4$ above 620 K have been estimated by extrapolation of the function of equation (9).

A measure of the volume thermal expansion for $CaMoO_4$ in the range 12–1300 K can be calculated from the expression

$$\left(\frac{\Delta V}{V}\right)_P = \int_{T_1}^{T_2} \beta(T)\,dt \tag{10}$$

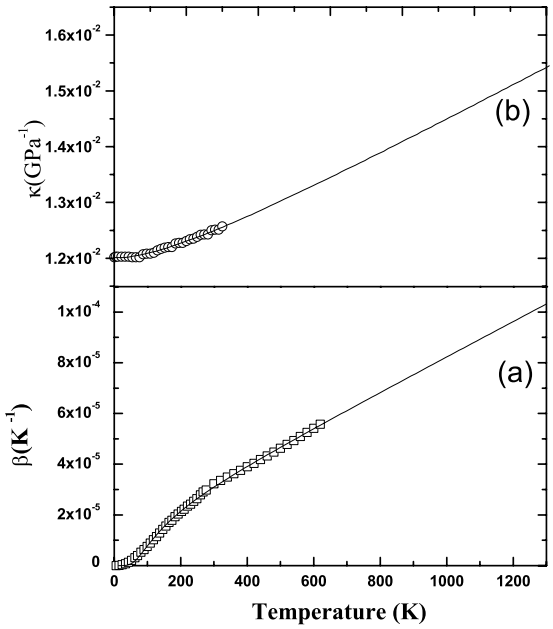


**Figure 5.** (a) The volume thermal expansion coefficient $\beta$ for $CaMoO_4$ in the range 4.2–620 K. The points in the region 300–620 K correspond to values determined from lattice constant measurements [26], while those in the region 4.2–300 K are derived from Debye temperature data [27] for isomorphous $CaWO_4$ normalized to the $CaMoO_4$ value at 300 K. The solid line represents a least-squares fitting of all these points (up to 620 K) to the function of equation (9) and an extrapolation of this function above 620 K; see the text for details. (b) The volume compressibility $\kappa$ for $CaMoO_4$ in the region 4.2–300 K. The points are derived from measurements of the elastic constants $c_{ij}$ in this region for isomorphous $CaWO_4$ [27] normalized to the corresponding measured $c_{ij}$-values of $CaMoO_4$ [28] at 300 K. The solid curve represents a least-squares fitting of these points (up to 300 K) to the function of equation (12) and a linear extrapolation above 300 K; see the text for details.

**Table 3.** Fitting values of the parameters for the functions in equations (9) and (12).

| | |
|---|---|
| $\beta(T)$ | $E = 0.0023 \pm 0.0001$, $F = 0.47 \pm 0.05$ (K), $T_0 = 181 \pm 5$ (K) |
| $\kappa(T)$ | $G = 0.0111 \pm 0.0004$ ($GPa^{-1}$), $H = (3.48 \pm 0.43) \times 10^{-6}$ ($GPa^{-1}$ $K^{-1}$), $L = 270 \pm 70$ (K) |

by using the fitted data of figure 5(a) and bearing in mind the definition of $\beta(T)$. It has been found that $(\Delta V/V)_P \approx 7\%$ for this range.

Regarding the volume compressibility, there are measured values of the elastic constants $c_{ij}$ for $CaMoO_4$ only at room temperature [28]. On the other hand, the elastic constants $c_{ij}$ for isomorphous $CaWO_4$ have been measured [27] in the region 4.2–300 K, thus enabling us to normalize them to the room temperature $c_{ij}$-values of $CaMoO_4$. These procedures of normalization (interpolation) of the experimental thermal expansion coefficient and compressibility data for $CaWO_4$ to corresponding data for $CaMoO_4$ are justified because the measured values of these quantities for the two isomorphous materials are quite close.

The determination of elastic constants and compressibilities is based on ultrasonic velocity measurements [27, 28] and, therefore, the resulting values of these quantities are adiabatic. In contrast, the Raman scattering (at a given temperature) is an isothermal process. However, the difference between adiabatic and isothermal elastic constants for such dielectric crystals [27]

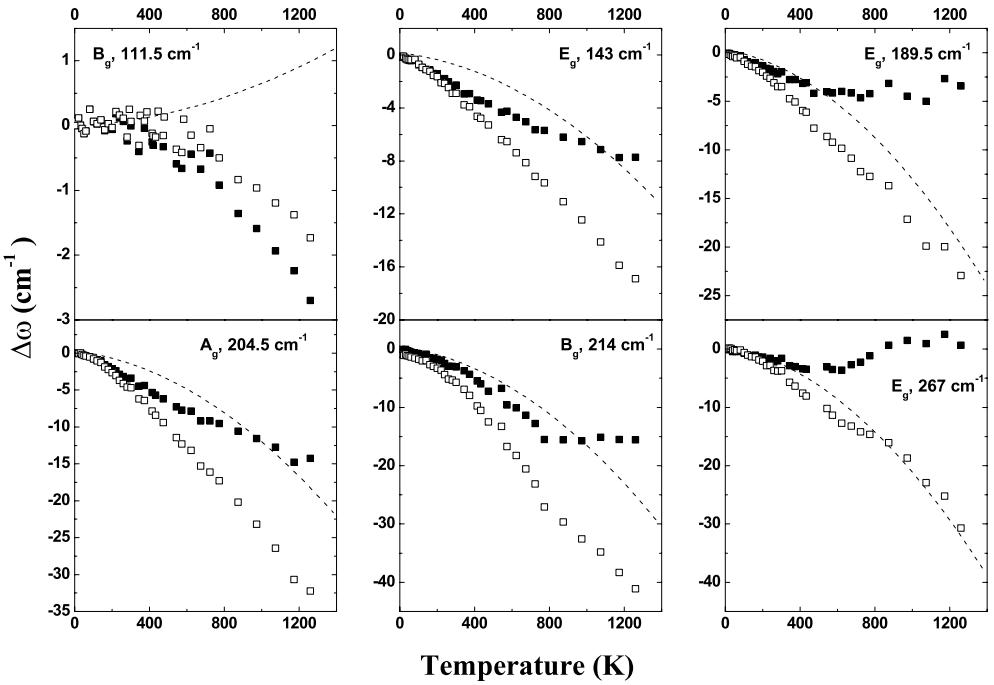


**Figure 6.** Volume expansion $\Delta\omega_{vol}$ (- - - -) and pure temperature anharmonic $\Delta\omega_{anh}$ (■) contributions to the total frequency shift $\Delta\omega_{tot}$ (□) for the six external modes of $CaMoO_4$ as functions of temperature. The error bars for all shifts are up to ±10%.

is less than 1% at 300 K and negligible at 10 K; this can be easily verified by an expression [29] relating the two sets of elastic constants and the linear thermal expansion coefficients.

The volume compressibility $\kappa(T)$ can be calculated from the elastic constants $c_{ij}$ using the formula [29]

$$\kappa = \frac{c_{11} + c_{12} + 2c_{33} - 4c_{13}}{(c_{11} + c_{12})c_{33} - 2c_{13}^2} \tag{11}$$

valid for tetragonal symmetry crystals. The values of $\kappa(T)$ obtained from equation (11) have been fitted to the function [23, 25]

$$\kappa(T) = G + HT + \frac{HL^2}{L + T} \tag{12}$$

and the data for the range 4.2–300 K have been extrapolated for $T > 300$ K assuming an almost linear dependence of $\kappa(T)$ at high $T$, an assumption which is reasonable bearing in mind that this is the situation in other dielectric crystals [21, 22] and that the variation of $\kappa$ with $T$ is generally very small in most crystals. The data points and the resulting fit are shown in figure 5(b), while the fitting parameters $G$, $H$ and $L$ are given in table 3.

*3.2.3. Contributions of the volume and pure temperature effects to the observed total frequency shifts in $CaMoO_4$.* Equations (4) have been used to separate the contributions of the volume and pure temperature effects and equation (5) to calculate the frequency shift $\Delta\omega_{vol}$ due to volume thermal expansion. This analysis has been possible for all 13 Raman phonons of $CaMoO_4$ and the results are shown in figure 6 for the external modes and figure 7 for the internal ones.

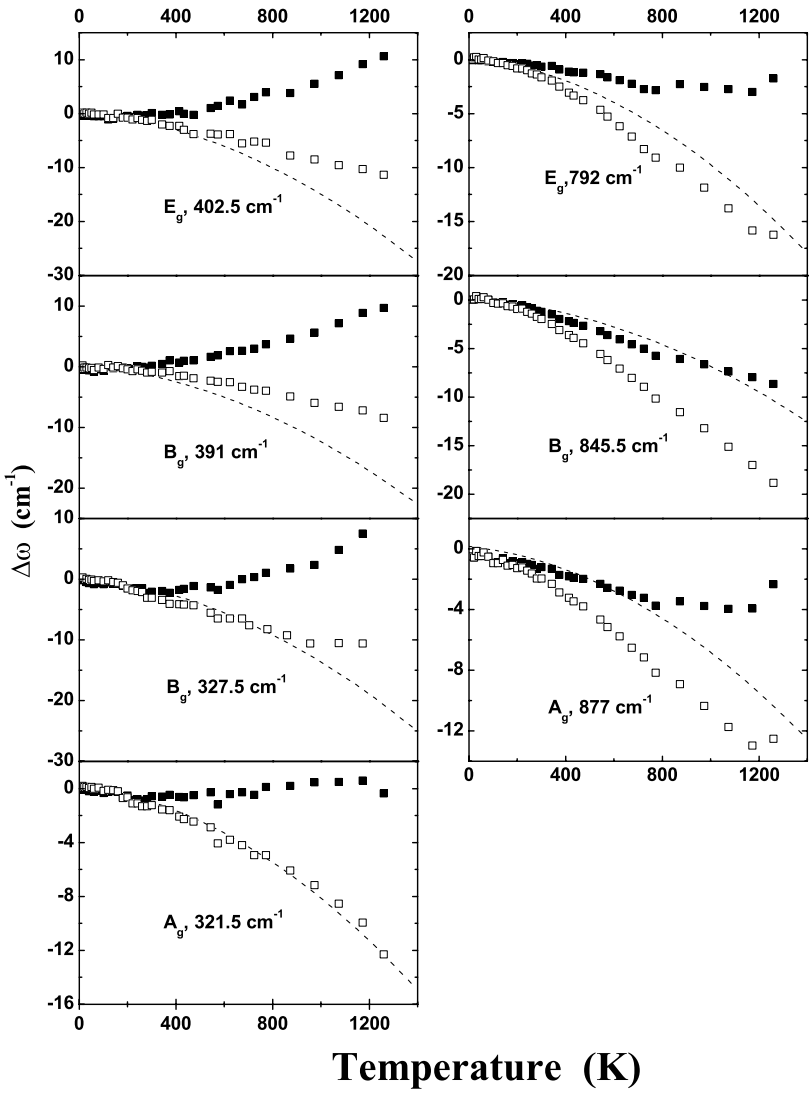


**Figure 7.** Volume $\Delta\omega_{vol}$ (- - - -) and anharmonic $\Delta\omega_{anh}$ (■) contributions to the total frequency shift $\Delta\omega_{tot}$ (□) for the seven internal modes of $CaMoO_4$ as functions of temperature. The error bars for all shifts are up to ±10%.

In three of the external modes (those at 143, 204.5 and 214 $cm^{-1}$) the contributions of the volume-induced and anharmonic shifts are comparable and of the same sign (negative). The modes at 189.5 and 267 $cm^{-1}$ show strong downward volume contributions, but only marginal anharmonic shift contributions; in fact, the former shows initially, up to about 600 K, a slight downward anharmonic shift and negligible one above this temperature, while the latter after a small initial downward shift displays a likewise upward anharmonic shift, thus bringing the overall (i.e., over the entire $T$-range) anharmonic contribution to the total shift close to zero. Finally, in the lowest-frequency external mode at 111.5 $cm^{-1}$, the two contributions are small and of opposite sign—that is, an upward volume-induced shift and a downward anharmonic one, with the latter being larger in absolute value.

Turning our attention to the internal modes, we notice that all modes display a downward volume-induced shift. The modes at 792, 845.5 and 877 $cm^{-1}$ show also a downward shift due to the anharmonic effect which is weaker than (792, 877 $cm^{-1}$) or comparable to (845.5 $cm^{-1}$) the volume-induced one. In three internal modes at 327.5, 391 and 402.5 $cm^{-1}$ the shifts caused by the two effects have opposite sign, but in all of them the volume-induced shift is greater, in absolute terms, than that due to the anharmonic effect. In the remaining seventh internal mode at 321.5 $cm^{-1}$, the anharmonic contribution to the total shift is negligible.

From the results shown in figures 6 and 7, it is evident that in most cases (8 out of the 13 phonons) and above a certain temperature (which varies between 300 and 800 K, depending on the phonon), the volume-induced shift is greater than the pure temperature (anharmonic) one. For three phonons at 143, 204.5 and 214 $cm^{-1}$, though, the anharmonic contribution seems to be slightly higher than the volume one up to a $T$ of about 900 K, while for the phonon at 845.5 $cm^{-1}$ the two contributions are comparable throughout the $T$-range. The phonon at 111.5 $cm^{-1}$ is a special case which has been discussed above. According to the model proposed by Weinstein and Zallen [20], for ionic solids, the thermal expansion (volume) effect dominates the overall shift with $T$, as the vibrational modes involve atomic species with non-overlapping electronic configurations; in contrast, for covalent solids, in which substantial electronic overlaps exist, the volume effect is relatively reduced so the shifts induced by the two effects become comparable, with the anharmonic contribution being higher than the volume one in most cases. Therefore, if we assume the validity of this model [20], we conclude that the character of bonding (responsible for the vibrational spectrum) in $CaMoO_4$ is predominantly ionic.

## 4. Conclusions

The temperature dependence for Raman-active phonons of tetragonal $CaMoO_4$ has been studied over a wide range of temperatures (12–1300 K). Above a certain temperature, which varies between 400 and 600 K depending on the phonon, both the frequency and the linewidth of all 13 Raman phonons display almost linear temperature dependence, implying that three-phonon processes (rather than the four-phonon ones) dominate the anharmonic phonon decay and broadening at high temperatures. The lowest-frequency $B_g$ phonon at 111.5 $cm^{-1}$ (attributed to translational motions of $MoO_4^{2-}$ units against each other) is temperature independent in the region 12–400 K and, having in mind its abnormal softening with pressure [8], it is concluded that the two contributions to the total frequency shift with temperature, i.e. the contributions due to the volume (expansion) and pure temperature effects, have opposite signs and are counterbalanced. The reduced $(\partial\omega/\partial T)/\omega$ slopes of the high-frequency phonons are about an order of magnitude smaller than those of the low-frequency ones, thus confirming the division internal (former)/external (latter) which has been adopted [2, 8] for the Raman modes of $CaMoO_4$. There is no evidence of phonon discontinuities or instabilities with temperature, indicating that $CaMoO_4$ is stable throughout the temperature range of study.

From the combination of the temperature-dependent Raman results of this study and previous Raman data for $CaMoO_4$ under variable hydrostatic pressure [8], we have performed an anharmonicity analysis in order to separate and calculate the volume and pure temperature contributions to the total frequency shift with temperature. The results of this analysis show that, in most cases, the total shift is dominated by the volume effect, suggesting that the bonding in $CaMoO_4$ is mainly ionic in character.

## Acknowledgments

We are grateful to Dr A Jayaraman and AT&T Bell Laboratories for making available single crystals of $CaMoO_4$.

## References

[1] Wyckoff R W G 1965 *Crystal Structures* vol 3, 2nd edn (New York: Interscience) p 21
[2] Porto S P S and Scott J F 1967 *Phys. Rev.* B **157** 716
[3] Kaminskii A A 1990 *Laser Crystals* 2nd edn (Berlin: Springer)
[4] Nicol M and Durana J F 1971 *J. Chem. Phys.* **54** 1436
[5] Ganguly N and Nicol M 1977 *Phys. Status Solidi* b **79** 617
[6] Jayaraman A, Batlogg B and Van Uitert L G 1983 *Phys. Rev.* B **28** 4774
[7] Jayaraman A, Batlogg B and Van Uitert L G 1985 *Phys. Rev.* B **31** 5423
[8] Christofilos D, Kourouklis G A and Ves S 1995 *J. Phys. Chem. Solids* **56** 1125
[9] Desgreniers S, Jandl S and Carlone C 1984 *J. Phys. Chem. Solids* **45** 1105
[10] Suda S and Sato T 1997 *J. Phys. Soc. Japan* **66** 1707
[11] Basiev T T, Sobol A A, Voronto Y K and Zverev P G 2000 *Opt. Mater.* **15** 205
[12] Scott J F 1968 *J. Chem. Phys.* **48** 874
[13] Liegeois-Duyckaerts M and Tarte P 1972 *Spectrochim. Acta* A **28** 2037
[14] Scott J F 1968 *J. Chem. Phys.* **49** 98
[15] Raptis C 1983 *J. Phys. E: Sci. Instrum.* **16** 749
[16] Balkanski M, Wallis R F and Haro E 1983 *Phys. Rev.* B **28** 1928
[17] Ipatova I P, Maradudin A A and Wallis R F 1967 *Phys. Rev.* **155** 882
[18] Peercy P S 1973 *Phys. Rev.* B **8** 6018
[19] Cerdeira F, Mello F E A and Lemos V 1983 *Phys. Rev.* B **27** 7716
[20] Weinstein B A and Zallen R 1984 *Light Scattering in Solids* vol 4, ed M Cardona and G Guntherodt (Heidelberg: Springer) pp 463–527
[21] Liarokapis E, Anastassakis E and Kourouklis G A 1985 *Phys. Rev.* B **32** 8346
[22] Raptis Y S, Kourouklis G A, Anastassakis E, Haro E and Balkanski M 1987 *J. Physique* **48** 239
[23] Cai J, Raptis C, Raptis Y S and Anastassakis E 1995 *Phys. Rev.* B **51** 201
[24] Perakis A, Sarantopoulou E, Raptis Y S and Raptis C 1999 *Phys. Rev.* B **59** 775
[25] Sarantopoulou E, Raptis Y S, Zouboulis E and Raptis C 1999 *Phys. Rev.* B **59** 4154
[26] Deshpande V T and Suryanarayana S V 1969 *J. Phys. Chem. Solids* **30** 2484
[27] Gluyas M, Hughes F D and James B W 1973 *J. Phys. D: Appl. Phys.* **6** 2025
[28] Farley J M, Saunders G A and Chung D Y 1975 *J. Phys. C: Solid State Phys.* **8** 780
[29] Nye J F 1985 *Physical Properties of Crystals* 2nd edn (Oxford: Oxford University Press)